Effects of Carbon-Supported Nickel Catalysts on MgH2 Decomposition

ARTICLE *in* THE JOURNAL OF PHYSICAL CHEMISTRY C · MARCH 2008

Impact Factor: 4.77 · DOI: 10.1021/jp711749h

Effects of Carbon-Supported Nickel Catalysts on MgH_2 Decomposition

M. A. Lillo-Ródenas,*,†,‡ K. F. Aguey-Zinsou,† D. Cazorla-Amorós,‡ A. Linares-Solano,‡ and Z. X. Guo†

Department of Chemistry, University College London, London WC1H 0AJ, United Kingdom, and Grupo de Materiales Carbonosos y Medio Ambiente, Departamento de Química Inorgánica, Facultad de Ciencias, Universidad de Alicante, Ap. 99, E-03080, Alicante, Spain

Received: December 14, 2007; In Final Form: January 21, 2008

This paper analyzes the improvement of MgH_2 decomposition by the addition of nickel-based catalysts, mostly carbon-supported nickel catalysts. Our study shows that some experimental parameters such as the catalyst content, its composition, the method of preparation, and milling time strongly affect its activity toward MgH_2 decomposition. We observe that carbon-supported nickel catalysts have superior performance than those just containing carbon and nickel physically mixed and, especially, than those containing only nickel. This emphasizes the role played by carbon and by the nickel−carbon interaction on the activity of such MgH_2-based materials. A decrease, followed by differential scanning calorimetry (DSC), in the decomposition temperature of MgH_2 of 150 °C can be achieved with some selected supported catalysts. Suitable selection of the catalyst preparation conditions leads to materials for which decomposition of 6.6 wt % hydrogen occurs in just 9 min at 300 °C, in comparison to 240 min required for undoped MgH_2, and is stable after five cycles. Comparison between catalysts supported on different carbon materials having similar compositions but different nickel particle size shows no relevant differences in their isothermal decomposition kinetics.

1. Introduction

Developing a practical hydrogen storage system has become increasingly important for the commercialization of fuel-cell-powered vehicles. Various options are under investigation, but none has met the combined stringent demands on hydrogen storage capacity, operation temperature, safety, and cost.[1]

Magnesium (Mg) is a very attractive material for hydrogen storage due to its abundance, low cost, low density, high theoretical gravimetric H_2 density of 7.6 wt %, and high volumetric H_2 density of 110 g/L.[2] It satisfies most of the requirements for storage medium in stationary as well as in mobile applications.[3] However, practical applications are impeded by the high decomposition temperature of magnesium hydride and by its slow kinetics. Numerous studies have been carried out to identify suitable Mg-based systems that desorb hydrogen at temperatures low enough to use the exhaust-gas waste heat from vehicles.[3] Considerable progress has been made in the use of powder processing techniques to accelerate the decomposition kinetics by mechanical alloying and the incorporation of different additives or catalysts.

The effects of carbon additives on magnesium-based systems have been reported by several groups.[4−10] Others have focused on the introduction of different metals,[5,11−20] metal oxides,[6,21−27] metallic compounds,[6,28] metallic nanoparticles,[25,29−31] and carbon-supported metals[32] to the hydride.

Among the different catalysts studied, nickel has attracted considerable attention due to its active role in the dissociation of hydrogen.[13] Thus, Bogdanovic et al.[11] concluded that nickel-doped materials possess excellent cyclic stability and high hydrogenation/dehydrogenation rates.

Liang et al.[12] analyzed the hydrogen desorption of MgH_2 milled with 5 at. % of different metals: Ti, V, Mn, Fe, and Ni. These authors compare the MgH_2 decomposition at 300 °C for 10 min in the undoped and doped materials, and they show that no decomposition takes place in the undoped samples, whereas 5 wt % hydrogen is decomposed in the doped samples within 3−10 min, depending on the metallic additive. The efficiency of the metals on the hydride decomposition follows the order Ti > V > Fe > Ni > Mn.

Berlouis et al.[13] report that adding 0.1−10 at. % Ni to Mg shows no evidence of the formation of Mg_2Ni and small differences in the decomposition kinetics of the hydride. The authors also note that the catalytic activity of nickel decreases with hydriding/dehydriding cycling, leading to a reduction in the levels of absorbed/desorbed hydrogen.

Tessier and Akiba[14] show that introduction of 1 at. % nickel lowers the differential scanning calorimetry (DSC) decomposition peak from 443 to 423 °C due to the reduction in the activation energy for the decomposition.

Bobet et al.[15] studied the system Mg + 10 wt % metal (Co, Ni, or Fe), showing different features: (i) the transition metal is well-dispersed in magnesium and no agglomeration is observed; (ii) the amount of hydrogen from the decomposition cycles is below the expected theoretical amount; and (iii) depending on the milling conditions (i.e., under Ar or H_2), the amount of hydrogen recovered after the first and second decomposition cycles is coincident or not.

Recently, Hanada et al.[25,29] analyzed the effects of 1 and 2 wt % nanoparticles of iron, cobalt, nickel, and copper on MgH_2. The results show that the decomposition of MgH_2 is strongly improved after addition of a small amount of the nanoparticles.[25,29] The decomposition of 6.5 wt % hydrogen from pure MgH_2 takes around 6 h at 300 °C, whereas only 4 h is required at 160 °C in the presence of 2 wt % nickel nanoparticles.[25,29]

* Corresponding author: tel +34965909350; fax +34965903454; e-mail mlillo@ua.es.
† University College London.
‡ Universidad de Alicante.

10.1021/jp711749h CCC: $40.75
Published on Web 03/22/2008

TABLE 1: Summary of Carbon Samples Used in the Study

sample	type of material and commercial reference	company
G	graphite, general purpose	Fisher Chemical Co.
MWCNT	multiwall carbon nanotubes[34]	CAER, University of Kentucky
NF	carbon nanofiber GANF	Grupo Antolín Ingeniería S.A.
AC	activated carbon, A1100 10x25	Mead Westvaco
ACF	activated carbon fiber ACT-25	Nippon Kynol Inc. Gun Ei Chemical Industry

However, results from the second cycle are slightly worse than those for the first one, probably due to the formation of Mg_2Ni in the boundary between the MgH_2 and Ni phases.[25,29] Kojima et al.[30] have demonstrated that 4.9−5.8 wt % hydrogen can be desorbed at 150−200 °C within 6 h from a nanocomposite of magnesium with nano-Ni/Al_2O_3/C.

Varin et al.[19,20] compared the effects of different types of nickel, including nanometric, submicrometric, and micrometric nickel particles. They conclude that the addition of 2 wt % Ni is beneficial for both the hydrogen absorption and desorption steps.[19] For desorption, the DSC temperature is reduced between 30 and 50 °C, and as an example, 5 wt % H_2 is recovered in 16 min at 300 °C using the micro- and submicrometric nickel catalysts.[19] They also study co-doped MgH_2 by micro/nanometric nickel and nano-oxides (Al_2O_3 and Y_2O_3), showing that only Y_2O_3 has a limited effect on the decomposition of MgH_2 containing nickel.[20] Yoo et al.[32] studied a complex MgH_2 system cocatalyzed by $Ba_3(Ca_{1+x}Nb_{2-x})O_{9-\delta}$ (BCN) proton-conductive ceramics and nanoparticle bimetallic Ni/Pd catalyst supported on single-wall carbon nanotubes (SWCNT). This system shows a significant enhancement of the hydrogen sorption kinetics at 230−300 °C, in comparison with MgH_2 and MgH_2 catalyzed by BCN.[32] Only 12 min is required for decomposition of the best Mg-based materials at 300 °C.[32] Jensen et al.[18] have followed the kinetics of pure and nickel-doped MgH_2 by in situ time-resolved powder X-ray diffraction, and they show that the activation energy for decomposition of MgH_2 is lower for the nickel-doped samples, in agreement with previous findings.[19,20]

All the above results have shown that the decomposition of MgH_2 is largely influenced by nickel and the size of the nickel particles. The best results have been shown by the introduction of nanometric nickel. However, no cyclic stability is shown for this nickel size.

In this study we focus on Mg-based systems prepared by ball milling, with the incorporation of carbon-supported nickel, encouraged by the positive effects of Ni-containing carbon nanofibers on MgH_2.[33] The use of carbon-supported nickel has never been explored before, although it might be a very interesting approach for the stabilization of nickel particles of nanometric size and could lead to Mg-based systems that are stable with cycling.

2. Experimental Section

2.1. Precursors. MgH_2 powder was purchased from Th. Goldschmidt AG, with a nominal composition of 95 wt % MgH_2 and 5 wt % Mg and an average diameter of 50 μm. Several carbon materials were selected as nickel supports. Table 1 summarizes the nomenclature and key features of the carbon materials. $Ni(NO_3)_2{\cdot}6H_2O$ was used as a Ni precursor and was purchased from Fluka (pa). Elemental nickel from Sigma−Aldrich, 3 μm in diameter, was also used for the preparation of some samples. This material is referred to as micrometric nickel.

2.1.1. Porosity Characterization of Carbon Supports. These carbon supports were characterized by physical adsorption of gases (N_2 and CO_2 at −196 and 0 °C, respectively) using an Autosorb 6-B apparatus (Quantachrome Corp.). Nitrogen adsorption was conducted at −196 °C to determine the total volume of micropores (pore size <2 nm) using the Dubinin−Radushkevich equation and to determine the apparent Brunauer−Emmett−Teller (BET) surface area. CO_2 adsorption was carried out at 0 °C to assess the narrowest micropores (pore size <0.7 nm) also by use of the Dubinin−Radushkevich equation.[35,36]

2.1.2. Metal Content Analysis of Carbon Supports. The content of the metallic impurities in the carbon materials to be used as supports was quantified by inductively coupled plasma optical emission spectrometry (ICP-OES) (Perkin−Elmer Optima 4300) after extraction of the metals from the carbon materials in HNO_3 for 7 days.

2.1.3. Oxidation of Carbon Supports. Prior to impregnation with the nickel precursor, the carbon samples were oxidized in a H_2O_2 solution of 30 wt % in water from Sigma−Aldrich. Each carbon sample (2 g) was added to 20 mL of the hydrogen peroxide solution, which was then stirred for 2 h. The samples were then washed in distilled water and dried overnight in an oven at 110 °C. The nomenclature of these samples includes "-ox".

2.2. Catalyst Preparation. Carbon-supported nickel catalysts were prepared by excess-solution impregnation for 48 h, as previously described in the literature.[37] The oxidized carbon material (2 g) was mixed with 50 mL of $Ni(NO_3)_2{\cdot}6H_2O$ solution, at two different concentrations of nickel, to obtain 20 and 40 wt % (nominal) nickel contents, respectively. Afterward, the samples were dried overnight at 110 °C.

2.3. Catalyst Reduction. The reduction temperature of selected catalysts was studied by temperature-programmed reduction (TPR) with evolved gas analyzed by mass spectrometry (Balzers, Omnistar). A sample of about 10 mg of catalyst precursor was exposed to 5% H_2/Ar gas mixture at 90 mL min^{-1} (BOC gases) and warmed up at a heating rate of 5 °C min^{-1} up to 600 °C (see Figure 1 as an example). These experiments showed that temperatures around 400 °C were sufficient to reduce all the nickel present in the catalysts.

All the materials were reduced in pure H_2 under the following experimental conditions: 1 g of catalyst was heated to 500 °C at 5 °C min^{-1} and then held for 5 h under a hydrogen flow rate of 90 mL min^{-1} (BOC gases, 99.99% purity) during the whole reduction process.

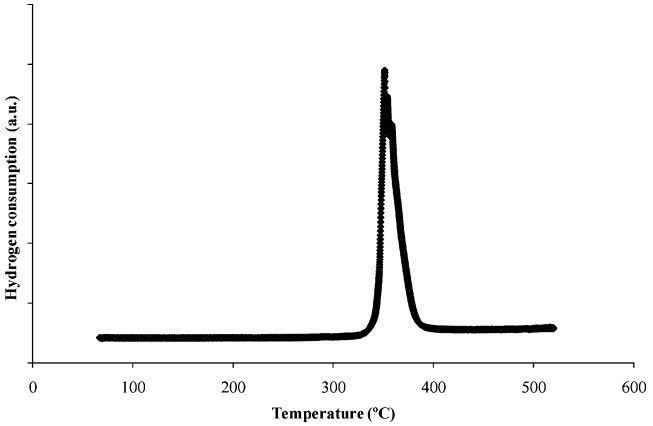

Figure 1. TPR experiment of Ni/G-ox sample.

2.4. Metal Content of the Catalysts. The metallic content of the prepared catalysts was determined by ICP-OES on a Perkin−Elmer Optima 4300 after extraction of the metals from the carbon materials in HNO_3 for 7 days.

2.5. Milling Conditions. Three groups of Ni catalysts were used. The first involved carbon-supported nickel, the second used micrometric nickel as a catalyst, and the third contained a mixture of carbon and micrometric nickel.

Before being mixed with any catalyst, MgH_2 powder was premilled under 4 bar of argon for 15 h in a Fritsh P5 planetary ball mill in sealed pots. The samples were weighed in a glove box filled with high-purity argon. Each experiment involved about 10 g of MgH_2 and 38 stainless-steel balls of 10 mm in diameter, leading to a ball-to-powder weight ratio of 15:1. A relatively low milling speed of 300 rpm was selected.

For the first group of samples, the carbon-supported nickel catalysts were mixed with the premilled MgH_2 in the presence of 5 or 10 wt % of the 20 wt % Ni carbon-supported catalysts, leading to a nickel content of 1 and 2 wt % and a carbon content of 4 and 8 wt %, respectively. In addition, one sample was prepared with 5 wt % of the 40 wt % Ni carbon-supported catalyst, resulting in final nickel and carbon contents of 2 and 3 wt %, respectively.

For the second type of samples, micrometric nickel was used as a metallic source and two different contents were tested, 1 or 2 wt % Ni.

Finally, the third type of MgH_2-based samples comprised 2 wt % micrometric Ni and 8 wt % carbon, where the nickel is not supported on carbon but just physically mixed with carbon and the hydride.

The samples were milled for times ranging from 5 min to 20 h in a high-energy SPEX 8000 mill (1080 cycles/min) under argon. In each case, 2 g of powder were milled with stainless steel balls of 10 mm leading to the same ball-to-powder weight ratio of 15:1. The same milling procedure was applied to the premilled MgH_2, from 5 min to 20 h, as references.

Nomenclature of the different samples is as follows: Samples prepared by impregnation and reduction (first type) are named as wt % Ni/wt % carbon/MgH_2. Thus, sample 2% Ni/8% G-ox/MgH_2 was prepared by introducing graphite-supported nickel to the MgH_2, and the approximate nickel and graphite weight percentages in the mixture are 2% and 8%, respectively. The nomenclature of samples prepared by mixing and milling MgH_2 with micrometric nickel (second type) include the percentage of nickel: that is, 2% Ni + MgH_2 was prepared by mixing and milling 2 wt % micrometric nickel with MgH_2. The materials comprising carbon, micrometric nickel, and MgH_2 (third type) are referred to as wt % Ni + wt % carbon + MgH_2. As an example, 2% Ni + 8% G-ox + MgH_2 was prepared by mixing the appropriate amounts of each component.

2.6. Temperature-Programmed Decomposition. The effect of carbon-supported nickel catalysts on the decomposition temperature of MgH_2 was determined by simultaneously coupled thermogravimetry (TG), differential scanning calorimetry (DSC) (Setsys-Setaram), and mass spectrometry (MS) (Omnistar, Balzers). A heating rate of 5 °C min^{-1} was used and the experiments were performed under an Ar flow rate of 90 mL min^{-1} (BOC gases, 99.999% purity). TG−DSC−MS was performed by use of sample weights in the range of 2−4 mg. The DSC curves were normalized for comparison purposes and they have been used to provide information about the decomposition temperature of the hydride.

2.7. Isothermal Decomposition. Hydrogen titration in different samples was performed on volumetric equipment (Pct-Pro 2000, Hy-Energy) under high-purity hydrogen (BOC gases, 99.999% purity). Around 100 mg of each sample was used in each case. Desorption measurements were performed between 275 and 300 °C and at 0.1 kPa.

TABLE 2: Porosity Characterization and Metallic Content of Carbon Samples[a]

sample	BET ($m^2 \cdot g^{-1}$)	DR N_2 ($cm^3 \cdot g^{-1}$)	DR CO_2 ($cm^3 \cdot g^{-1}$)	P (wt %)	Fe (wt %)	Ni (wt %)
G	13	0.01	0			
MWCNT	47	0.02	0		2.88	
NF	178	0.06	0.03			7.50
AC	1757	0.67	0.36	1.97		
ACF	1907	0.90	0.60			

[a] BET, Brunauer−Emmett−Teller surface area; DR N_2, total micropore volume (pore diameter below 2 nm) characterized by the Dubinin−Radushkevich equation; DR CO_2, narrow micropore volume (pore diameter below 0.7 nm) characterized by the Dubinin−Radushkevich equation.

2.8. Morphology and Structural Characterizations. The morphology of the carbon-supported nickel catalysts was analyzed by transmission electron microscopy (TEM) on a JEOL JEM-2010 high-tilt instrument operating at 200 kV with a structural spatial resolution of 0.5 nm.

The catalysts were characterized by X-ray diffraction (XRD) on a Siemens D5000 powder diffractometer equipped with a Cu Kα X-ray source, a graphite monochromator, and an internal standard of silicon powder. Diffraction data were collected by step scanning with a step size of 0.05° 2θ and a scan step time of 3 s. For each sample, at least two diffraction patterns were obtained, with different representative batches of samples for each run, in order to evaluate the reproducibility of the bands obtained. Identification of the species was computer-aided by use of JCPDF files.

3. Results and Discussion

3.1. Carbon Supports. As detailed in the Experimental Section, a wide range of carbon materials was selected as supports for preparation of the nickel catalysts. Table 2 shows the results for the porous texture characterization of such supports obtained by physical adsorption of gases, N_2 and CO_2 at −196 and 0 °C, respectively, as previously detailed. The table shows that the samples under study strongly differ in terms of porosity, covering materials from no apparent porosity to BET-specific surface areas in the range of 2000 m^2/g.

Metals in the carbon supports were identified and quantified by ICP and these results are also summarized in Table 2. Only carbon nanostructures, MWCNT and NF, incorporate iron and nickel, respectively, from their preparation catalysts. However, their metallic content is low. The AC contains some amount of phosphorus, since it was activated by phosphoric acid.

3.2. Carbon-Supported Nickel Catalysts. Different carbon-supported nickel catalysts were prepared and characterized by TEM. Figure 2 compiles some of the obtained images showing that, as expected, nickel dispersion is very different depending on the carbon support. Thus, G-ox, with very little surface area, shows the poorest nickel dispersion and some nickel particles of large size, even larger than 200 nm, are observed (Figure 2A). However, the mean nickel particle size for this catalyst is in the range of 50 nm.

The MWCNT-ox and NF-ox supports show good nickel dispersion, with the largest nickel particles in the range of 50 nm (Figure 2B,C) and the nickel mean particle size in the range of 15 nm. Note that some catalyst remains in the carbon nanostructures from their preparation procedure (iron-based for

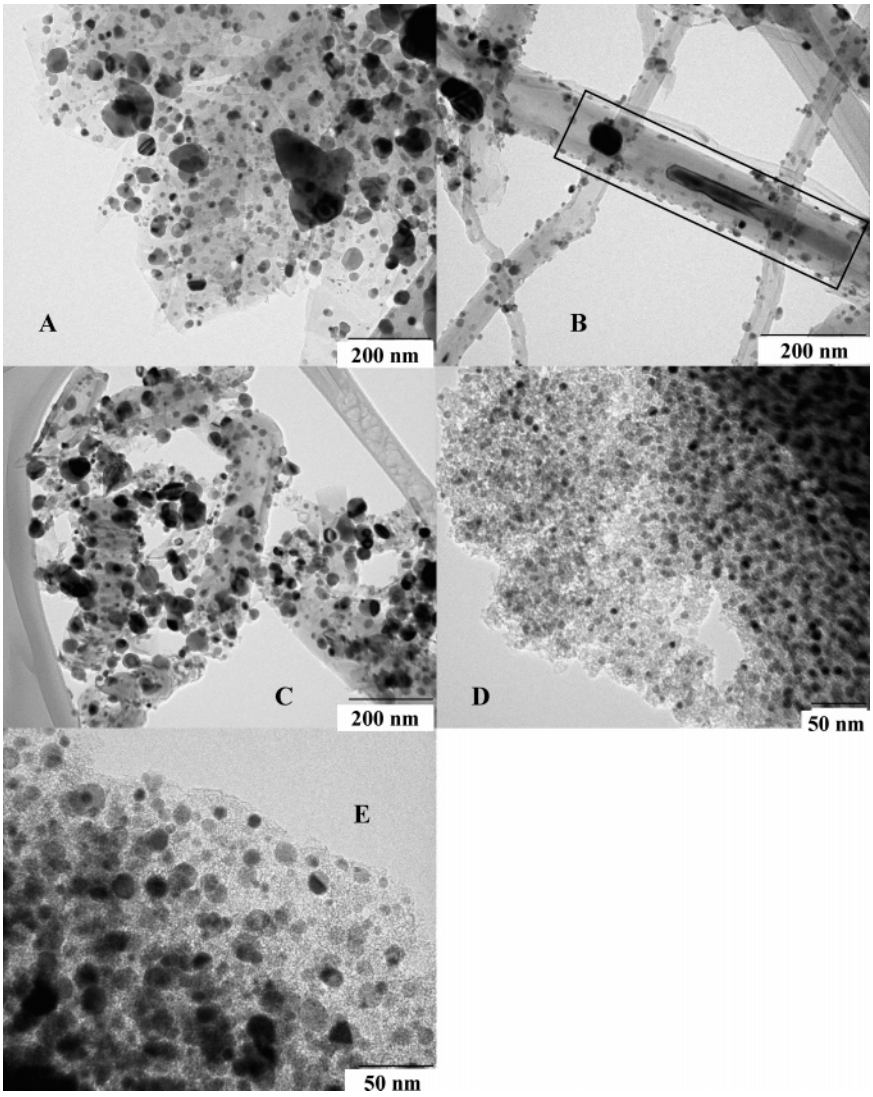

Figure 2. TEM images of different carbon-supported nickel catalysts with 20 wt % nickel nominal composition: (A) Ni/G-ox, (B) Ni/MWCNT-ox, (C) Ni/NF-ox, (D) Ni/AC-ox, and (E) Ni/ACF-ox.

MWCNT and nickel-based for NF), as seen from the TEM images (e.g., boxed area in Figure 2B).

The best nickel dispersion, as expected, occurs in those carbon materials with largest specific surface areas, AC and ACF. Thus, Figure 2 panels D and E show that there is very good nickel dispersion for these catalysts, with the largest nickel particles in the range of 15 nm and mean nickel particle size around 8 nm.

These carbon-supported nickel catalysts were also characterized by XRD and the diffraction patterns are shown in Figure 3. It is clear that the metallic nickel peaks exist in all the catalysts, indicative of the successful reduction of nickel in all the samples. The nickel crystalline size in the catalysts has been calculated by means of the Scherrer formula. The full width at half-maximum (fwhm) for the 44.3° 2θ peak was measured and a k value of 0.9 was used for these calculations. These results indicate that the mean crystalline size of nickel in the Ni/G-ox and Ni/ACF-ox catalysts is in the range of 20 nm, whereas this value decreases to 11 nm for the nickel in the other three catalysts.

The metallic content in the 20 wt % nominal Ni/carbon catalysts was characterized by ICP and these results are summarized in Table 3. As shown, the amount of nickel introduced in most samples is around 20 wt %, except that in

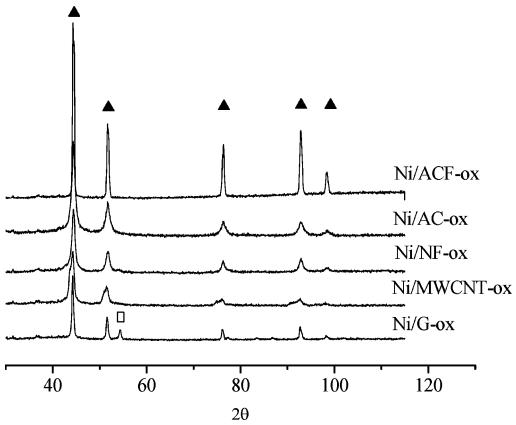

Figure 3. XRD patterns of the carbon-supported nickel catalysts with 20 wt % nickel nominal composition (▲, nickel peaks; □, graphite peaks).

Ni/MWCNT-ox, which is larger (around 27 wt %). In the case of Ni/NF-ox catalyst, the amount of nickel introduced is slightly lower than 20 wt %, although the total nickel content is in the range of 25 wt % due to the catalyst contained in the nanofibers from their preparation procedure.

3.3. Temperature-Programmed Decomposition. The dehydriding behaviors of the different MgH_2-based materials were

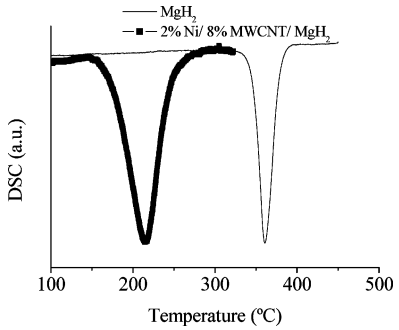

Figure 4. Comparison between decomposition of MgH_2 and 2% Ni/ 8% MWCNT/MgH_2, both milled for 15 min followed by DSC.

TABLE 3: Nickel Content for the Nickel-Supported Carbon Catalysts Prepared for 20 wt % Nominal Nickel

sample	Ni introduced (wt %)	total nickel (wt %)
Ni/G-ox	23	23
Ni/MWCNT-ox	27	27
Ni/NF-ox	18	25
Ni/AC-ox	20	20
Ni/ACF-ox	19	19

characterized by TG−DSC−MS measurements at the experimental conditions previously discussed. For simplicity of discussion, TG and MS measurements are not presented but are referred to at the end of this section. Therefore, DSC data feature in this part of the discussion. Examples of these DSC curves are shown in Figure 4. From DSC, the temperatures for decomposition of MgH_2 samples prepared at different conditions are assessed and compiled in Table 4.

Premilled MgH_2 shows a clear endothermic DSC peak at 363 °C. This sample was further milled without any catalyst for times ranging from 0.5 to 20 h as references. For short milling times, up to 1 h, there was no change in the decomposition behavior in comparison with the premilled MgH_2 (see Table 4). However, for milling times longer than 2 h, two overlapped DSC peaks are observed. These data show that milling up to 2 h does not appreciably modify the decomposition behavior of the hydride, although beyond this time, higher decomposition temperatures are required for complete dehydriding. The appearance of the two peaks in the decomposition of MgH_2 has been previously reported in the literature as due to bimodal distribution of particle sizes in the initial stages of milling.[7]

Table 4 shows that the introduction of carbon-supported nickel catalysts with 1 wt % Ni leads to a decrease in the decomposition temperature of MgH_2, particularly for the AC-ox, NF-ox, and G-ox-supported catalysts at some selected milling conditions. Thus, for most carbon-supported nickel catalysts, the lowest decomposition temperatures occur after low to moderate milling, up to 60 min. Only for the ACF-ox-supported catalyst is the decomposition temperature lower after milling for 2 h.

Comparison between these data and those for the sample 1% Ni + MgH_2 (second type sample) shows that, for similar nickel contents, the decomposition temperature is lower for MgH_2 with the carbon-supported nickel catalyst than with the micrometric nickel, even for the low surface area graphite support. This result clearly indicates the role played by carbon on the improvement of MgH_2 decomposition, due to improved dispersion of nickel particles or reduced particle growth of MgH_2 during cycling.[33]

With increasing amounts of nickel, from 1 to 2 wt %, the decomposition temperature is further reduced. A decomposition peak temperature is observed at 217 °C for the Ni/MWCNT-containing sample. It must also be pointed out that all these materials present one decomposition peak for MgH_2, ascribed to a prevalent particle size (see Figure 4, which compares the normalized DSC for MgH_2 and 2% Ni/8% MWCNT/MgH_2, both milled for 15 min). The large reduction in the decomposition temperature of MgH_2, in the range of 150 °C, can be more clearly observed in the figure. Such a significant decrease in the decomposition temperature of the hydride followed by DSC has not been reported before, neither by the addition of carbon materials[33] nor by the addition of different Ni-based catalysts[13,14,18−20,32] or metallic oxides.[27]

The effect of two different carbon support percentages has been analyzed in two samples prepared by the same method and containing similar amounts of nickel but differing in the amount of carbon support, 2% Ni/8 % G-ox/MgH_2 and 2% Ni/ 3% G-ox/MgH_2. Table 4 shows that the decomposition temperature for the hydride is only slightly lower for that containing a higher amount of the G-ox support.

The decomposition temperature of MgH_2 in samples containing 2 wt % Ni supported on carbon has been compared to that prepared with 2 wt % micrometric nickel and MgH_2 (see Table 4). Although the introduction of 2 wt % micrometric nickel lowers the decomposition temperature of the hydride, in agreement with what was previously reported in the literature,[13,14,18] this temperature is significantly lower when nickel is supported on carbon, pointing out the convenience of using this new way of introducing nickel, supporting it on carbon.

To understand the reason for such improved performance of the carbon-supported nickel catalysts (also observed in the 1

TABLE 4: Peak Temperature of Decomposition, Determined by DSC, for Samples Milled for Different Periods of Time[a]

		DSC (°C) for milling time			
sample	type of material	5 min	15 min	60 min	120 min
MgH_2	*b*	362	361	361	360, 376*
1% Ni/4% G-ox/MgH_2	1		286*, 345	291	293
1% Ni/4% NF-ox/MgH_2	1	218, 269*	267	275	293
1% Ni/4% AC-ox/MgH_2	1		302*, 335	270	292
1% Ni/4% ACF-ox/MgH_2	1		337, 371*	300*, 365	275*, 345
2% Ni/8% G-ox/MgH_2	1		277	279	283
2% Ni/8% MWCNT-ox/MgH_2	1	221	217	245	270
2% Ni/8% NF-ox/MgH_2	1	259	242	263	286
2% Ni/8% AC-ox/MgH_2	1		260	260	290
2% Ni/3% G-ox/MgH_2	1		282	284	287
1% Ni + MgH_2	2		328, 366*	308*, 363	318*, 363
2% Ni + MgH_2	2		318, 364*	309*, 375	309, 367[c]
2% Ni + 8% G-ox + MgH_2	3		324, 370*	306*, 342	298

[a] The most intense peak is marked with an asterisk. [b] Control sample. [c] Both peaks have the same intensity.

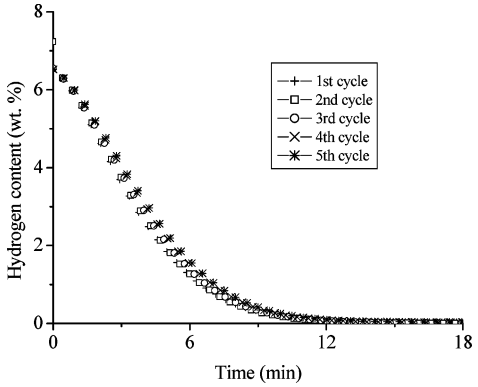

Figure 5. Decomposition kinetics for 2% Ni/8% NF-ox/MgH_2 milled for 15 min for five consecutive cycles.

TABLE 5: Peak Temperature of Decomposition for MgH_2 and for 1%Ni/4%G-ox/MgH_2 Milled for Different Periods of Time[a]

milling time (min)	DSC decomp peak for MgH_2 (°C)	
	in MgH_2 sample	in 1% Ni/4% G-ox/MgH_2 sample
15	361	286*, 345
60	361	291
120	360, 376*	293
1200	361*, 371	318*, 359
2400	364, 379*	344, 387*

[a] The most intense peak is marked with an asterisk.

wt % Ni samples), an additional sample was prepared by mixing 2 wt % micrometric nickel, 8 wt % G-ox, and MgH_2 (third type). It was milled under the same conditions as the rest of the samples. Comparison between this sample and a sample prepared by supported nickel on graphite with the same composition (sample 2% Ni/8% G-ox/MgH_2) shows that MgH_2 decomposes at a much lower temperature for the carbon-supported nickel sample, which further confirms the important effect of particle size of nickel on the decomposition temperature of MgH_2 or by the interaction between nickel and carbon when the catalyst is supported, that improves the interaction between the nickel catalyst and MgH_2. In this sense, the literature has shown that the amount of hydrogen chemisorbed on a Ni−carbon material is strongly dependent on nickel particle size and on the method of preparation of such materials. The mechanical mixture of nickel and graphite shows poor results.[38]

To optimize the milling conditions, the effect of milling time on the decomposition temperatures of catalyzed MgH_2 was also studied. The decomposition temperatures of MgH_2 in sample 1% Ni/4% G-ox/MgH_2 were measured and compared with those of pure MgH_2. Table 5 shows that milling beyond 120 min of the nickel-catalyzed samples leads to an increase in the decomposition temperature of MgH_2. This fact, also observed by other authors,[20] is likely due to cold welding of MgH_2 particles, which needs to be further explored.

3.4. Isothermal Decomposition. Decomposition kinetics of MgH_2 were characterized at 300 °C under 0.1 kPa of hydrogen for the different Mg-based materials. Also, some measurements at 290 and 275 °C were carried out for comparison.

Five cycles of dehydriding/hydriding of different MgH_2-based materials were studied in order to analyze the stability of the prepared materials. Figure 5 shows, as an example, the isothermal decomposition curves and the cyclability of the sample 2% Ni/8% NF-ox/MgH_2 after five cycles. The same behavior is observed in all other samples studied. The decomposition curves for MgH_2 indicate that 4 h is required for

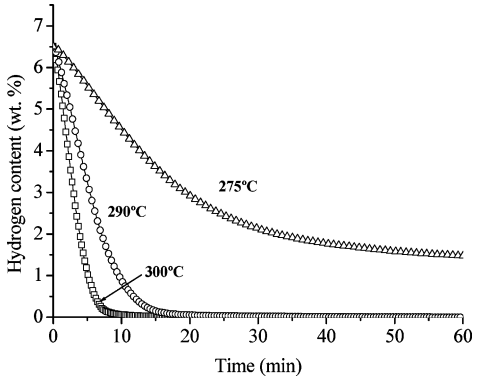

Figure 6. Effect of temperature on decomposition kinetics of magnesium hydride for 2% Ni/8% G-ox/MgH_2 sample.

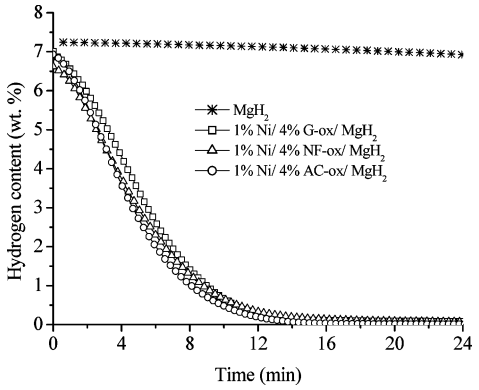

Figure 7. Comparison between decomposition kinetics of MgH_2 and some selected samples containing 1 wt % Ni supported on carbon milled for 60 min.

complete decomposition of the hydride at 300 °C for most of the milling conditions studied.[33]

3.4.1. Effect of Temperature on Decomposition Kinetics. The decomposition kinetics of selected samples were characterized at 275, 290 and 300 °C, as shown in Figure 6. As expected, decomposition becomes sluggish as the temperature decreases, although around 5 wt % hydrogen can be recovered at 275 °C in just 60 min for 2% Ni/8% G-ox/MgH_2. The plots for samples 2% Ni/8% MWCNT-ox/MgH_2 and 2% Ni/8% NF-ox/MgH_2 are very similar to those in Figure 6, with the decomposition kinetics being slower for samples having less catalyst content. The important effect of temperature on decomposition kinetics of MgH_2 has been previously reported for nickel-based catalysts[12,18−20] as well as for other materials.[31,41,39] The activation energy for dehydrogenation of magnesium hydride in sample 2% Ni/8% G-ox/MgH_2 has been calculated according to Arrhenius equation from data in Figure 6, leading to a value in the range of 180 kJ/mol. This value is lower than that for MgH_2 calculated in previous studies.[18]

In the following, the effects of different experimental variables on the decomposition of MgH_2 at 300 °C are discussed.

3.4.2. Effect of Carbon Support. Figure 7 presents the decomposition kinetics of samples containing 1 wt % nickel supported on three different carbon materials: graphite, nanofibers, and activated carbon. Decomposition kinetics of MgH_2 in these samples, milled for 60 min, are much faster than for bulk MgH_2 milled under the same conditions. Thus, only 15 min is required for complete decomposition of the hydride at 300 °C in these samples, and the amount of hydrogen recovered agrees well with what is theoretically expected from their composition.

Comparison between samples supported on different carbon materials in Figure 7 shows that only slight differences in

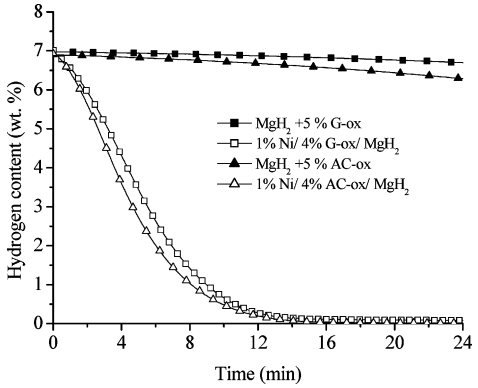

Figure 8. Comparison between decomposition kinetics at 300 °C of MgH_2 in samples containing either carbon materials or carbon-supported nickel catalysts.

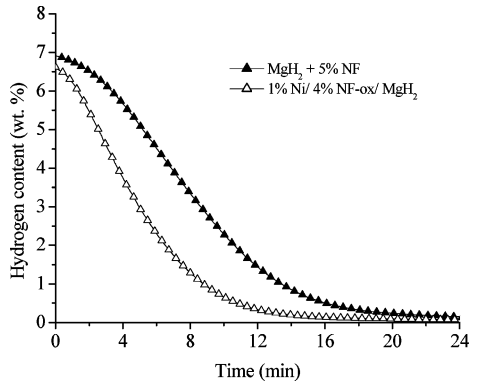

Figure 9. Comparison between decomposition kinetics at 300 °C of MgH_2 in the sample containing NF or NF-supported nickel catalysts.

decomposition of the hydride exist, despite the difference in the surface area of the supports and, particularly, in the size of the nickel particles deposited on them, as observed in Figure 2. This implies that, in the range of nickel particle sizes of the carbon-supported nickel catalysts, from 8 to 50 nm, there is not much difference between the activities of the catalysts. It must also be noted that the decomposition temperatures of samples in Figure 7, which vary by ~20 °C, do not lead to significant differences in the isothermal decomposition.

3.4.3. Importance of Supporting Nickel. Comparison was made between the samples containing carbon, from a previous work,[33] and those containing the carbon-supported nickel catalysts. Figure 8 plots the isothermal decomposition curves for two samples containing carbon-supported nickel catalysts and two samples containing just the carbon materials (from ref 33). As noted, a large improvement in the decomposition kinetics is obtained from the samples containing nickel catalysts, compared to samples containing just the carbon material.

In the case of NF, however, this difference is much less significant, due to its nickel content from its preparation procedure.[33] Nevertheless, as shown in Figure 9, some improvement in the decomposition kinetics occurs when nickel is supported on NF because the amount of nickel in 1% Ni/4% NF-ox/MgH_2 is around 3 times higher than that in the MgH_2 + 5 wt % NF sample.

To confirm the effect of the nickel catalyst content on the isothermal decomposition kinetics, supported materials containing twice the amount of catalyst (2 wt % Ni and 8 wt % carbon) were tested. Figure 10 compares the decomposition curves for the four materials containing carbon-supported nickel catalysts and that for MgH_2 as a reference. Note that not all the selected samples were prepared with the nickel content, and the best

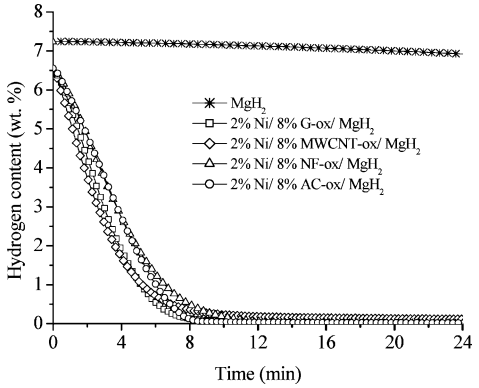

Figure 10. Comparison between decomposition kinetics of MgH_2 and some selected samples containing 2 wt % Ni supported on carbon (samples with MWCNT-ox and NF-ox were milled for 15 min, whereas those containing G-ox and AC-ox were milled for 60 min).

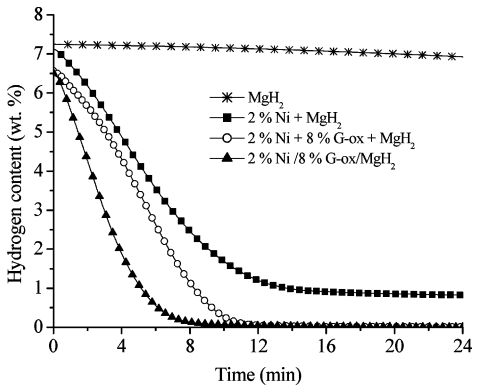

Figure 11. Comparison between decomposition kinetics of MgH_2 and samples containing 2 wt % Ni prepared in different conditions (note the micrometric size of nickel introduced in samples 2% Ni + MgH_2 and 2% Ni + 8% G-ox + MgH_2, whereas the nickel size in the catalyst used for preparation of MgH_2 + 2% Ni/8% G-ox is nanometric).

milling time for each support was selected according to the results obtained in the DSC measurements (Table 3).

This plot shows that MgH_2 isothermal decomposition kinetics is very fast at 300 °C in the samples containing the nickel catalysts. Only 9 min is required for total decomposition of the hydride, which implies a substantial decrease in time compared with the samples containing 1% Ni/4% carbon/MgH_2 (see Figure 7). This clearly shows the important effect of the amount of carbon-supported Ni catalyst on the decomposition kinetics of MgH_2.

The sample 2% Ni/8% MWCNT/MgH_2 shows improved properties in comparison with the other studied materials. Its faster decomposition should be attributed, especially, to its high nickel content, according to the data for the Ni/MWCNT catalyst from Table 3.

3.4.4. Effect of Catalyst Preparation Method. Figure 11 compares the MgH_2 decomposition for samples prepared from graphite-supported nickel (first type), micrometric nickel (second type), or mixed micrometric nickel and graphite (third type). The plots for MgH_2 and MgH_2 containing G-ox are also presented for comparison.

The best-performing sample corresponds to one prepared by impregnation with nickel nitrate followed by reduction in hydrogen (2% Ni/8% G-ox/MgH_2). As previously shown, the mean size of the nickel particles in this sample is in the range of 20 nm. The sample prepared with the same nickel composition but by mixing micrometric nickel (3 μm), G-ox, and the hydride displays slower decomposition kinetics. This shows the

importance of nickel particle size or the carbon−nickel interaction for its catalytic properties.

An additional sample prepared with the same amount of micrometric nickel (2 wt %), but in the absence of G-ox, shows much slower decomposition kinetics. Decomposition of MgH_2 in this sample is incomplete even after 2 h. These results clearly reveal the beneficial effect not only of the metal catalyst, in our case nickel, but also of the presence of carbon. The effect of carbon seems to be 2-fold: on one hand it allows an intimate contact between the catalyst and the MgH_2, and on the other hand carbon is inserted in the outer region of MgH_2 particles after milling and could work as a "pathway" favoring hydrogen diffusion from MgH_2 across the MgO layer surrounding the MgH_2 particles.[40]

The decomposition kinetics of Ni-doped MgH_2 has been previously studied in the literature.[12,13,25,29,30] Liang et al.[12] showed that the addition of 5 at. % (∼10 wt %) Ni to MgH_2 leads to 5 wt % hydrogen desorbed in 10 min at 300 °C. Varin et al.[19] reported the desorption of 5 wt % H_2 in 16 min at 300 °C in their 2 wt % Ni-based materials, whereas Yoo et al.[32] showed that around 12 min was required for 6 wt % hydrogen recovery for some of their materials at the same temperature. Compared with all these results, the samples prepared in this study show much improved performance, evolving 6.5 wt % hydrogen in 9 min.

Berlouis et al.[13] show that Mg-based materials containing different amounts of nickel become less active after cycling. Hanada et al.[25,29] report that the decomposition of MgH_2 catalyzed by nickel nanoparticles takes 4 h at 160 °C (1 and 2 wt %). However, the material is not stable, and decomposition kinetics for the second cycle is slower than for the first.[25,29] The reasons for such deactivation shown by several authors are not clear, although the authors assume that there is a decrease of both the absorption and desorption of the hydrogen with increasing cycles.[13] Regarding this point, the performance of our samples should also be outlined, because for the carbon-supported samples prepared in this study, no change in desorption kinetics is observed after cycling and the total decomposition of the hydride takes place during the tests.

Kojima et al.[30] have analyzed several nickel-containing materials, including a nanocomposite containing 5 wt % Ni. Their results show that the best MgH_2 decomposition kinetics, close to 6 wt % H_2 in 6 h at 200 °C, is shown by a nanocomposite material containing nano Ni, Al_2O_3, and C,[30] which underlines, in agreement with our results, the role played by carbon on the performance of the catalysts for the decomposition of MgH_2.

Moreover, the addition of carbon has also proved to be beneficial to hydrogen absorption of a nanocomposite Mg−V, where the percentage of desorbed hydrogen is close to the theoretical value when graphite is present, whereas it is lower without the graphite.[40] The addition of graphite also shows some beneficial effect on hydride formation kinetics.[41]

Comparison between our results in Figure 11 and those previously published for the Mg_2Ni−C system[42] shows that much faster decomposition kinetics at 300 °C is achieved by the use of carbon-supported nickel catalysts or just by the introduction of the nickel and carbon in the Mg-based material.

3.3.5. Effect of Carbon Content. The effect of carbon content on the carbon-supported catalysts has been studied by comparing the hydride decomposition kinetics for two samples with the same nickel content but different amounts of G-ox support. Figure 12 shows the favorable effect of carbon support; the sample containing a larger amount of the support shows faster decomposition kinetics.

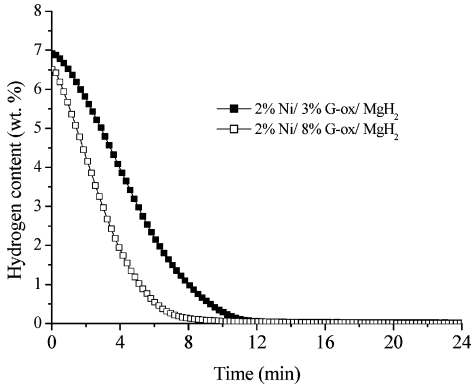

Figure 12. Comparison between decomposition kinetics of MgH_2 in two materials containing 2 wt % Ni that differ in the amount of G-ox support.

A possible explanation for this behavior may be related to a larger MgH_2 particle reduction during milling with a higher amount of carbon. Differences in the heat conduction of the samples could also play a role. Thus, a high carbon support content enhances the heat-conducting properties of the prepared materials, favorable for the dehydriding process.

4. Conclusions

This study shows that carbon-supported nickel catalysts improve the decomposition kinetics of MgH_2 to a higher level than nickel physically mixed with carbon or nickel alone. Small amounts of these catalysts, prepared by impregnation followed by reduction, are enough to reduce the decomposition time of magnesium hydride at 300 °C from 4 h to 9 min or to reduce the DSC decomposition peak by as much as 150 °C.

The porous texture of the carbon supports has shown, as expected, an important effect on the mean size of the nickel particles. However, this seems to have little effect on the catalytic role of the nickel; in this range of sizes, the activity of the carbon-supported catalysts is similar for similar nickel compositions with different carbon supports.

Milling time has an important effect on the catalyzed MgH_2-based materials. Thus, with MgH_2, a short period of milling, up to 1 or 2 h, is desirable for the decomposition of the hydride. The amount of nickel supported on carbon, from 1 to 2 wt % nominal, has also shown some effect on the decomposition of MgH_2. For similar amounts of nickel, the amount of carbon support has shown some influence: the catalysts containing a higher amount of carbon show slightly better performance.

Introduction of carbon considerably improves the decomposition kinetics of MgH_2, even if it is not in the form of carbon-supported catalysts but just by physical mixture. This outlines the importance of the composition of such catalysts and the fact that carbon must be one of their components. The larger MgH_2 particle reduction and/or improvement of the heat conduction properties of the prepared materials after the introduction of a larger amount of carbon may explain such behavior.

The carbon-supported samples show no reduction in the decomposition kinetics or the amount of hydrogen evolved after five dehydriding−hydriding cycles, in contrast to the samples just containing nickel and MgH_2, which show marked deactivation.

Temperature is important for the isothermal decomposition kinetics of the catalyzed materials: 60 min is required for 5 wt

% hydrogen recovery at 275 °C, whereas 9 min is sufficient for complete hydride decomposition at 300 °C.

Acknowledgment. M.A.L.R. thanks Generalitat Valenciana for postdoctoral fellowship (AEST06/002 and BEST/2007/214). We thank MEC (Project CTQ2006-08958/PPQ and ENE2005-23824-E/CON), Generalitat Valenciana (Accomp06/089), the EU (Feder), Hytrain (MRTN-CT-2004-512443), and the UK EPSRC (GR/S26965/01, GR/S52636/01) for financial support.

References and Notes

(1) Schlapbach, L.; Zuttel, A. *Nature* **2001**, *414*, 353.
(2) Hoffman, K. C.; Reilly, J. J.; Salzano, F. J.; Waide, C. H.; Wiswall, R. H.; Winsche, W. E. *Int. J. Hydrogen Energy* **1976**, *1*, 133.
(3) Selvam, P.; Viswanathan, B.; Swamy, C. S.; Srinivasan, V. *Int. J. Hydrogen Energy* **1986**, *11*, 169.
(4) Imamura, H.; Kusuhara, M.; Minami, S.; Matsumoto, M.; Masanari, K.; Sakata, Y.; Itoh, K.; Fukunaga, T. *Acta Mater.* **2003**, *51*, 6407.
(5) Huot, J.; Tremblay, M.-L.; Schulz, R. *J. Alloys Compd.* **2003**, *356*−*357*, 603.
(6) Güvendiren, M.; Baybörü, E.; Öztürk, T. *Int. J. Hydrogen Energy* **2004**, *29*, 491.
(7) Shang, C. X.; Guo, Z. X. *J. Power Sources* **2004**, *129*, 73.
(8) Lukashev, R. V.; Klyamkin, S. N.; Tarasov, B. P. *Inorg. Mater.* **2006**, *42*, 726.
(9) Wu, C. Z.; Wang, P.; Yao, X.; Liu, C.; Chen, D. M.; Lu, G. Q.; Cheng, H. M. *J. Alloys Compd.* **2006**, *414*, 259.
(10) Montone, A.; Grbovicì, J.; Bassetti, A.; Mirenghi, L.; Rotolo, P.; Bonetti, E.; Pasquini, L.; Antisari, M. V. *Int. J. Hydrogen Energy* **2006**, *31*, 2088.
(11) Bogdanovic, B.; Hofmann, H.; Neuy, A.; Reiser, A.; Schlichte, K.; Spliethoff, B.; Wessel, S. *J. Alloys Compd.* **1999**, *292*, 57.
(12) Liang, G.; Huot, J.; Boily, S.; Van Neste, A.; Schulz, R. *J. Alloys Compd.* **1999**, *292*, 247.
(13) Berlouis, L. E. A.; Cabrera, E.; Hall-Barientos, E.; Hall, P. J.; Dodd, S.; Morris, S.; Imam, M. A. *J. Alloys Compd.* **2000**, *305*, 82.
(14) Tessier, P.; Akiba, E. *J. Alloys Compd.* **2000**, *302*, 215.
(15) Bobet, J.-L.; Akiba, E.; Darriet, B. *Int. J. Hydrogen Energy* **2001**, *26*, 493.
(16) Charbonnier, J.; De Rango, P.; Fruchart, D.; Miraglia, S.; Pontonnier, L.; Rivoirard, S.; Skryabina, N.; Vulliet, P. *J. Alloys Compd.* **2004**, *383*, 205.
(17) Tran, N. E.; Lambrakos, S. G.; Imam, M. A. *J. Alloys Compd.* **2006**, *407*, 240.
(18) Jensen, T. R.; Andreasen, A.; Vegge, T.; Andreasen, J. W.; Ståhl, K.; Pedersen, A. S.; Nielsen, M. M.; Molenbroek, A. M.; Besenbacher, F. *Int. J. Hydrogen Energy* **2006**, *31*, 2052.
(19) Varin, R. A.; Czujko, T.; Wasmund, E. B.; Wronski, Z. S. *J. Alloys Compd.* **2007**, *432*, 217.
(20) Varin, R. A.; Czujko, T.; Wasmund, E. B.; Wronski, Z. S. *J. Alloys Compd.* **2007**, *446*−*447*, 63.
(21) Oelerich, W.; Klassen, T.; Bormann, R. *J. Alloys Compd.* **2001**, *315*, 237.
(22) Dehouche, Z.; Klassen, T.; Oelerich, W.; Goyette, J.; Bose, T. K.; Schulz, R. *J. Alloys Compd.* **2002**, *347*, 319.
(23) Bobet, J.-L.; Desmoulins-Krawiec, S.; Grigorova, E.; Cansell, F.; Chevalier, B. *J. Alloys Compd.* **2003**, *351*, 217.
(24) Barkhordarian, G.; Klassen, T.; Bormann, R. *Scr. Mater.* **2003**, *49*, 213.
(25) Hanada, N.; Ichikawa, T.; Fujii, H. *J. Alloys Compd.* **2005**, *404*−*406*, 716.
(26) Aguey-Zinsou, K.-F.; Ares Fernandez, J. R.; Klassen, T.; Bormann, R. *Mater. Res. Bull.* **2006**, *41*, 1118.
(27) Aguey-Zinsou, K.-F.; Ares Fernandez, J. R.; Klassen, T.; Bormann, R. *Int. J. Hydrogen Energy* **2007**, *32*, 2400.
(28) Delchev, P.; Himitliiska, T.; Spassov, T. *J. Alloys Compd.* **2006**, *417*, 85.
(29) Hanada, N.; Ichikawa, T.; Fujii, H. *J. Phys. Chem. B* **2005**, *109*, 7188.
(30) Kojima, Y.; Kawai, Y.; Haga, T. *J. Alloys Compd.* **2006**, *424*, 294.
(31) Xu, X.; Song, C. *Appl. Catal., A* **2006**, *300*, 130.
(32) Yoo, Y.; Tuck, M.; Kondakindi, R.; Seo, C.-Y.; Dehouche, Z.; Belkacemi, K. *J. Alloys Compd.* **2007**, *446*−*447*, 84.
(33) Lillo-Ródenas, M. A.; Guo, Z. X.; Aguey-Zinsou, K. F.; Cazorla-Amorós, D.; Linares-Solano, A. *Carbon* **2008**, *46*, 126.
(34) Andrews, R.; Jacques, D.; Rao, A. M.; Derbyshire, F.; Qian, D.; Fan, X.; Dickey, E. C.; Chen, J. *Chem. Phys. Lett.* **1999**, *303*, 467.
(35) Cazorla-Amorós, D.; Alcañiz-Monje, J.; de la Casa-Lillo, M. A.; Linares-Solano, A. *Langmuir* **1998**, *14*, 4589.
(36) Linares-Solano, A.; Alcañiz-Monje, J.; Salinas-Martínez de Lecea, C.; Cazorla-Amorós, D. *Tanso* **1998**, *185*, 316.
(37) Silva, L. M. S.; Órfão, J. J. M.; Figueiredo, J. L. *Appl. Catal., A* **2001**, *209*, 145.
(38) Zhong, Z. Y.; Xiong, Z. T.; Sun, L. F.; Luo, J. Z.; Chen, P.; Wu, X.; Lin, J.; Tan, K. L. *J. Phys. Chem B* **2002**, *106*, 9507.
(39) Maddalena, A.; Petris, M.; Palade, P.; Sartori, S.; Principi, G.; Settimo, E.; Molinas, B.; Lo Russo, S. *Int. J. Hydrogen Energy* **2006**, *31*, 2097.
(40) Friedrichs, O.; Sánchez-López, J. C.; López-Cartes, C.; Klassen, T.; Bormann, R.; Fernández, A. *J. Phys. Chem. B* **2006**, *110*, 7845.
(41) Bouaricha, S.; Dodelet, J.-P.; Guay, D.; Huot, J.; Schulz, R. *J Mater. Res.* **2001**, *16*, 2893.
(42) Bobet, J.-L.; Grigorova, E.; Khrussanova, M.; Khristov, M.; Stefanov, P.; Peshev, P.; Radev, D. *J. Alloys Compd.* **2004**, *366*, 298.